A Fast Averaging Synchronization Algorithm for Clock Oscillators in Nonlinear Dynamical Network with Arbitrary Time-delays

CHEN Jie[1, 2] YU Miao[1, 2] DOU Li-Hua[1, 2] GAN Ming-Gang[1, 2]

Abstract This paper investigates the synchronization problem of clock oscillators in nonlinear dynamical network with arbitrary time-delays. First, a dynamic synchronization algorithm based on consensus control strategy, named fast averaging synchronization algorithm (FASA), is presented to find a solution to the synchronization problem. This algorithm can compensate the clock skew and offset differences between clock nodes, achieving the synchronization of clock nodes in a shorter time as compared to previous synchronization methods. Second, because of the dynamical performance of FASA, it is characterized from the perspective of compartmental dynamical system with arbitrary time-delays. In this case, the algorithm guarantees the states of all clock nodes in dynamical network converge to Lyapunov stable equilibria. Finally, numerical simulations and experimental results demonstrate the correctness and efficiency of the FASA, which means that the clock nodes can reach global consensus, and the synchronization error can reach nanosecond order of magnitude.

Key words Clock synchronization, dynamical network, arbitrary time-delays, consensus algorithm
DOI 10.3724/SP.J.1004.2010.00873

The clock synchronization in nonlinear dynamical network is extremely useful to coordinate activities between cooperating processors. The accuracy and convergence rate are two important factors of clock synchronization. Synchronization of clock nodes in dynamical network raises several difficulties[1−5]. First, in the real world, the environmental pressure, ambient temperature, varying frequencies and humidity fluctuation over time make the synchronization of clock oscillators more challenging. Second, some clock oscillator nodes in nonlinear dynamical network cannot communicate directly with each other, and they have to achieve the communication by multi-hop. In this case, it is impossible to choose an internal reference node to which the other nodes can be synchronized. Third, due to the unpredictable time-delays between clock oscillator nodes, the delivery time of messages is subject to random variation. In fact, the magnitude of delays can be larger than the required precision of synchronization. Finally, several nodes may be able to communicate with only a small subset of all clock nodes. Also, the communication links between clock nodes may fail over time.

The contribution of this paper is to develop a fast global dynamic algorithm that solves the synchronization problem of clock oscillator nodes connected through the nonlinear dynamical network with random time-delays. The rest of the paper is organized as follows. In Section 1, we present a survey on available literature related to the subject of synchronization of clock oscillator nodes in dynamical network. The mathematical model of clock oscillators and synchronization problem of clock oscillators in dynamical network, as well as some preliminaries, are given in Section 2. The proposed fast averaging synchronization algorithm (FASA) based on consensus control strategy and its convergence analysis are presented in Section 3. Simulation results are demonstrated and analyzed in Section 4. Section 5 concludes the paper.

1 Related work

In one aspect, the synchronization of clock oscillators in dynamical network shares much similarity with the "consensus" problem put forward in the research field of multi-agents[6−7]. In networks of multi-agents, "consensus" problem means to reach an agreement regarding a certain quantity of interest that depends on the state of all agents. A consensus algorithm is an interaction rule that specifies the information exchange between an agent and all of its neighbors in the network. Clock oscillators and clock time can be viewed as agents and common quantity of interest, respectively. Therefore, it is reasonable and natural to develop consensus algorithm for solving the synchronization problem of clock oscillators in dynamical network with time-delays. The synchronization of clock oscillators in dynamical network under variable time-delays was recently studied in [8]. Also, there have been different strategies proposed to solve the clock synchronization problem in dynamical network. One common approach is the flooding time synchronization protocol (FTSP)[9], which models the network as a rooted tree. Another approach is called the reference broadcast synchronization (RBS) scheme[10]. In this protocol, a reference clock node is selected to synchronize the other nodes in a cluster. Reference clock nodes in different clusters are synchronized together and act as gateways by converting local clock nodes in one cluster into those in another cluster. However, RBS scheme suffers from large overhead which is necessary to divide the dynamical network into clusters and to elect the reference clock nodes, and it is fragile to clock node failures. Furthermore, a fully distributed communication topology in which there are no special nodes such as roots or gateways was employed to overcome the disadvantage of FTSP and RBS. One example of a distributed synchronization strategy is the reachback firefly algorithm (RFA), inspired by firefly synchronization mechanism[11]. But this approach could not compensate clock skew. Then, Solis et al.[12] proposed the distributer time synchronization protocol (DTSP), which is fully distributed and can compensate the skews and offsets of clock oscillators. DTSP is formulated as a distributed gradient descent optimization problem. Compared with DSTP, the FASA proposed in this paper is also fully distributed and includes the offset and skew compensation of clock oscillators.

From another perspective, the clock oscillators in dynamical network are always highly interconnected and interdependent. Such system is commonly referred to as nonnegative dynamical system in [13]. A subclass of nonnegative dynamical systems are called compartmental systems[14−15]. Each compartmental system is assumed to be kinetically homogeneous, that is, any material entering the compartment is instantaneously mixed with that of the compartment. To describe the evolution of the

Manuscript received June 11, 2009; accepted July 20, 2009
Supported by National Science Fund for Distinguished Young Scholars (60925011)
1. School of Automation, Beijing Institute of Technology, Beijing 100081, P. R. China 2. Key Laboratory of Complex System Intelligent Control and Decision of the Ministry of Education, Beijing Institute of Technology, Beijing 100081, P. R. China

aforementioned dynamical systems accurately, it is necessary to include some information of the past system states in a mathematical model. The system state at a given time involves a piece of trajectories which are defined in continuous functions. And these functions can be viewed as an interval in the nonnegative or that of the state space. Thus, it is natural to put such theory to time-delayed dynamical systems[16]. Nonnegative and compartmental models are also widely used in the agreement problems by using directed graphs[17−19]. We believe that the convergence analysis that utilizes the properties of nonnegative and compartmental models combined with directed graph will shed light on the performance of synchronization algorithm in the dynamical network of clock oscillators.

2 Problem formulation and preliminaries

2.1 Clock model and clock synchronization

Consider the nonlinear dynamical network with random time-delays, which is depicted in Fig. 1.

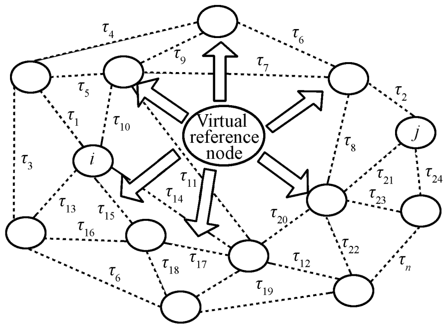

Fig. 1 The structure of clock oscillator nodes in nonlinear dynamical network with time-delays

Every clock node i has its own local state whose dynamics is given by[20−21]

$$\xi_i(t) = \alpha_i + \beta_i \cdot t + \gamma_i \cdot t^2 + \Delta_t \tag{1}$$

where $\xi_i(t)$ denotes the local clock oscillator reading; α_i is the local clock offset; β_i is the local clock skew which determines the clock oscillator speed; γ_i is the clock drift. Furthermore, Δ_t represents the clock jitter, which is modeled as zero mean white Gaussian noise with standard deviation σ_n, n is the number of clock nodes, $i = 1, \cdots, n$.

In the following sections, to find the solutions to main clock parameters by dynamic algorithm, for convenience we will restrict ourselves to a simplified model where the quadratic term in (1), often referred to as clock aging[22], is neglected. The clock jitter Δ_t also has little influence on the clock reading. Therefore, we denote the clock value at time t:

$$\xi_i(t) = \alpha_i + \beta_i \cdot t \tag{2}$$

Usually, the absolute reference time t is not available in each node, so it is impossible to compute the parameters α_i and β_i. However, we can obtain these indirectly by measuring the local clock of node i with respect to node j . If we solve (2) for t and put it into the equation for oscillator node j, we can get:

$$\xi_j = \alpha_{ij} + \beta_{ij} \cdot \xi_i \tag{3}$$

As a matter of fact, the "virtual" reference clock node to which we want to synchronize all nodes is denoted by

$$\xi_v(t) = \alpha_v + \beta_v \cdot t \tag{4}$$

Remark 1. The selected "virtual" reference node is fictitious, and the exact values of $(\alpha_v,\ \beta_v)$ are not important. What really concerns here is that all clock nodes converge to one common "virtual" reference node. Also, the parameters $(\alpha_v,\ \beta_v)$ depend on the initial condition and the dynamical network topology, which will be mentioned in Section 3.

Every local clock node keeps an estimate of the virtual time from (4) using a linear function described as follows:

$$\hat{\xi}_i = \hat{o}_i + \hat{s}_i \cdot \xi_i \tag{5}$$

As depicted in Fig. 1, we want to find $(\hat{s}_i,\ \hat{o}_i)$ for every oscillator node in dynamical system such that

$$\lim_{t\to\infty} \hat{\xi}_i(t) = \xi_v(t), \quad i = 1, \cdots, n \tag{6}$$

That is, all clock nodes will have a common global reference and will get synchronized soon. Fig. 2 shows the dynamic process of compensation for synchronization errors of each clock node in detail. FASA estimates how fast the local clock node to be synchronized is running with respect to the reference clock node and then it uses the value to compensate for the synchronizing clock, which is shown in Fig. 2. By using the clock skew and offset compensations, it is possible to keep each node synchronized for long periods of time.

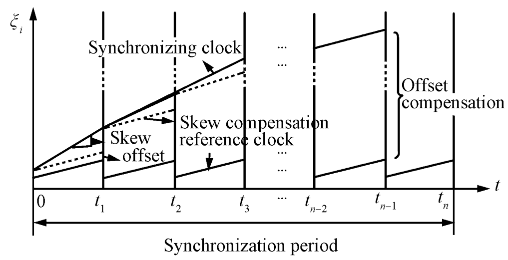

Fig. 2 The dynamic synchronization process of each clock node by using FASA

According to Fig. 2, we can convert linear equation (1) into a first-order system in the same segmental interval:

$$\dot{\xi}_i(t) = f(\xi_i(t)) \tag{7}$$

where $f \in \mathbf{R}$ is Lipschitz continuous and smooth and $f(0) = 0,\ t_k \le t < t_{k+1},\ k = 0, \cdots, n-1,\ i = 1, \cdots, n.$

For each clock oscillator node, we substitute (2) into (5), and the previous expression can be written differently as:

$$\hat{\xi}_i(t) = \hat{s}_i\beta_i \cdot t + \hat{s}_i\alpha_i + \hat{o}_i \tag{8}$$

$$\lim_{t\to\infty} \hat{s}_i(t) = \frac{\beta_v}{\beta_i} \tag{9}$$

$$\lim_{t\to\infty} \hat{o}_i(t) = \alpha_v - \hat{s}_i(t) \cdot \alpha_i = \alpha_v - \frac{\beta_v}{\beta_i} \cdot \alpha_i, \quad i = 1, \cdots, n \tag{10}$$

Remark 2. Solving the synchronization problem of clock nodes is a dynamic process whose network trajectories are characterized by the dynamical system (7). The goal is to establish a dynamic algorithm that enables a group of clock nodes in a network to agree upon certain quantities of interest with directed information flow which maybe delayed.

2.2 Preliminaries

As mentioned in Section 1, directed graphs are used to represent the dynamical network, and Section 1 have presented solutions to the consensus problem for the network with graph topologies and unknown random time-delays. For convenience, notations in this paper are summarized in Table 1.

Table 1 Notations

Symbols	Meaning
$\mathbf{R}^n$	n-dimensional Euclidean space
$\bar{\mathbf{R}}^n_+$	Nonnegative orthants of $\mathbf{R}^n$
$\mathbf{R}^n_+$	Positive orthants of $\mathbf{R}^n$
$\boldsymbol{x} \geq\geq \mathbf{0}, \boldsymbol{x} \in \mathbf{R}^n$	Every component of $\boldsymbol{x}$ is nonnegative
$\boldsymbol{x} \gg \mathbf{0}, \boldsymbol{x} \in \mathbf{R}^n$	Every component of $\boldsymbol{x}$ is positive
$A \geq\geq 0, A \in \mathbf{R}^{n\times m}$	Nonnegative matrix
$A \gg 0, A \in \mathbf{R}^{n\times m}$	Positive matrix
$A \geq 0, A \in \mathbf{R}^{n\times n}$	Nonnegative definite matrix
$(\cdot)^{\mathrm{T}}$	Matrix transpose
$(\cdot)^D$	Drazin generalized inverse
$\Vert \cdot \Vert$	Euclidean vector norm
$\mathcal{G} = (\mathcal{V}, \mathcal{E}, \mathcal{A})$	Weighted directed graph
$\mathcal{V} = \{1, \cdots, n\}$	Set of vertices
$\mathcal{E} \subseteq \mathcal{V} \times \mathcal{V}$	Direction of information flow
$\mathcal{A}_{(i,j)} = a_{ij} > 0$	Weighted adjacency matrix
a_{ij}	Weight of each edge

Following definitions are necessary for the convergence analysis of clock synchronization algorithm.

Definition 1. The dynamical network $\mathcal{G}$ with time-delays takes the following form:

$$\dot{\boldsymbol{\xi}}(t) = \boldsymbol{f}(\boldsymbol{\xi}(t)) + \boldsymbol{f}_d(\boldsymbol{\xi}(t-\tau_1), \cdots, \boldsymbol{\xi}(t-\tau_{nd}))$$
$$\boldsymbol{\xi}(\theta) = \boldsymbol{\phi}(\theta), \quad -\tau^* \leq \theta \leq 0, \quad t \geq 0 \tag{11}$$

where $\boldsymbol{f}_d : \mathbf{R}^n \times \cdots \times \mathbf{R}^n \to \mathbf{R}^n$ is locally Lipschitz continuous, $\boldsymbol{f}_d(0, \cdots, 0) = \mathbf{0}, \tau^* = \max_{i\in\{1,\cdots,n_d\}} \tau_i, i = 1, \cdots, n_d$ and the vector $\boldsymbol{\xi}(t) = [\xi_1(t), \cdots, \xi_n(t)]^{\mathrm{T}}$ is the state of networked clock nodes; $\boldsymbol{\phi}(\cdot) \in \mathbf{C} = \mathbf{C}([-\tau^*, 0], \mathbf{R}^n)$ is a continuous vector-valued function and satisfies the initial state of (11).

Definition 2. The clock synchronization problem is a dynamic process involving the trajectories of dynamical network described by the dynamical system:

$$\dot{\boldsymbol{\xi}}(t) = \boldsymbol{u}(t), \quad \boldsymbol{\xi}(0) = \boldsymbol{\xi}_0, \quad t \geq 0 \tag{12}$$

where $\boldsymbol{u}(t) = [\boldsymbol{u}_1(t), \boldsymbol{u}_2(t) \cdots, \boldsymbol{u}_n(t)]^{\mathrm{T}}$ is a clock synchronization algorithm. $\boldsymbol{u}_i(t)$ represents each input component of $\boldsymbol{u}(t), i = 1, \cdots, n$. And $\boldsymbol{u}_i(t)$ depends on the states of clock nodes i and its neighbors.

In a sense, the synchronization problem deals with the design of a clock synchronization algorithm $\boldsymbol{u}(t)$ such that $\hat{\xi}_i(t)$ satisfies (6). Due to the presence of directional constraints on information flow and system time-delays, $\boldsymbol{u}_i(t)$ is constrained to the feedback form $\boldsymbol{u}_i(t) = \boldsymbol{f}_i(\xi_i(t), \xi_{j_1}(t-\tau_{ij_1}), \cdots, \xi_{j_{mi}}(t-\tau_{ij_{mi}}))$, where $\tau_{ij_k} > 0$, $j_k \in \mathbf{N}_i = \{j \in \{1, \cdots, n\} : (j, i) \in \mathcal{E}\}$ are unknown communication time-delays between node i and node j_k. It is usually defined that $\tau_{ij} = 0$ if $(j, i) \notin \mathcal{E}$.

Definition 3. The nonlinear time-delay dynamical system (11) is a compartmental dynamical system if $\boldsymbol{F}(\cdot)$ is compartmental with $\boldsymbol{F}(\boldsymbol{\xi}(t)) = \boldsymbol{f}(\boldsymbol{\xi}(t)) + \boldsymbol{f}_d(\overbrace{\boldsymbol{\xi}(t), \boldsymbol{\xi}(t), \cdots, \boldsymbol{\xi}(t)}^{n})$, where $\boldsymbol{f}(\cdot)$ and $\boldsymbol{f}_d(\cdot) = [\boldsymbol{f}_{d1}, \boldsymbol{f}_{d2} \cdots, \boldsymbol{f}_{dn}]^{\mathrm{T}}$ are given by

$$\boldsymbol{f}_i(\boldsymbol{\xi}(t)) = -\sum_{j=1, j\neq i}^{n} a_{ji}(\boldsymbol{\xi}(t))$$
$$\boldsymbol{f}_{di}(\boldsymbol{\xi}(t-\tau_1), \cdots, \boldsymbol{\xi}(t-\tau_{n_d})) = \sum_{j=1, j\neq i}^{n} a_{ji}(\boldsymbol{\xi}(t-\tau_{ij})) \tag{13}$$

$a_{ij}(\boldsymbol{\xi}(\cdot)) \geq 0, \boldsymbol{\xi}(\cdot) \in \mathbf{C}_+$, $i \neq j$, $i, j \in \{1, \cdots, n\}$ denotes the instantaneous rate of material flow from the j-th to the i-th compartment; and $\tau_{ij}, i \neq j$, $i, j \in \{1, \cdots, n\}$ denotes the transfer time of material flow from the j-th to the i-th compartment.

From above, the form of nonlinear dynamical network $\mathcal{G}$ with time-delays can be written as:

$$\boldsymbol{u}(t) = \dot{\boldsymbol{\xi}}(t) = f(\boldsymbol{\xi}(t)) + \sum_{i=1}^{n_d} f_{d_i}(\boldsymbol{\xi}(t-\tau_i))$$
$$\boldsymbol{\xi}(\theta) = \boldsymbol{\phi}(\theta), \quad -\tau^* \leq \theta \leq 0, \quad t \geq 0 \tag{14}$$

where $\boldsymbol{f} : \bar{\mathbf{R}}^n_+ \to \bar{\mathbf{R}}^n_+$ is given by $\boldsymbol{f}(\boldsymbol{\xi}(t)) = [\boldsymbol{f}_1(\xi_1(t)), \boldsymbol{f}_2(\xi_2(t)), \cdots, \boldsymbol{f}_n(\xi_n(t))]^{\mathrm{T}}$, $\boldsymbol{f}(0) = \mathbf{0}$, $\boldsymbol{f}_{d_i} : \bar{\mathbf{R}}^n_+ \to \bar{\mathbf{R}}^n_+, i = 1, \cdots, n_d$, and $\boldsymbol{f}_d(0) = \mathbf{0}$. Furthermore, it is assumed that $\boldsymbol{f}_{d_i}(\cdot), i = 1, \cdots, n$ are strictly decreasing functions and $\boldsymbol{f}_{d_i}(0) = \mathbf{0}$.

3 Clock synchronization algorithm and its convergence analysis

3.1 Fast averaging synchronization algorithm

In this section, a clock synchronization algorithm, which is called FASA, is proposed and described. The main idea is to use a distributed consensus algorithm based on local information exchange. More explicitly, FASA forces all nodes to converge to a common "virtual" node as defined in (4) and implements the skew estimation, skew compensation, and offset compensation of clock oscillators in the dynamical network.

3.1.1 Relative clock skew estimation

FASA is concerned with estimating the relative clock skew β_{ij} of node i with respect to its neighbor j. It is assumed that the readings of the two local clock nodes are instantaneous and clock node j stores the current local time $\xi_j(t_1)$ into a communication packet, and then, node i receives this packet for a while and records its own local time $\xi_i(t_1)$. At the same time, each node i records the pair $(\xi_i(t_1), \xi_j(t_1))$. When a new information packet from node i reaches node j, the same operation is applied to get the new pair $(\xi_i(t_2), \xi_j(t_2))$.

Remark 3. By using media access control (MAC)-layer time-stamping in our experimental facilities of four oscillators which are shown in Section 4, it is easy to get the current local clock time $\xi_i(t_1)$, packet transmission, and reading of the local clock time $\xi_j(t_2)$ of node i. In the same way, we can get $\xi_i(t_2)$ and $\xi_j(t_1)$ of node j.

The estimation of β_{ij} is written as follows:

$$\mu_{ij_{\text{new}}} = \lambda_\mu \mu_{ij} + (1-\lambda_\mu)\frac{\xi_j(t_2)-\xi_j(t_1)}{\xi_i(t_2)-\xi_i(t_1)} \tag{15}$$

where $\mu_{ij_{\text{new}}}$ indicates the new value of variable μ_{ij}, and $\lambda_\mu \in (0,1)$ is a tuning parameter. If there is no measurement error and the skew is a constant, then μ_{ij} converges to β_{ij} as stated in the following theorem.

Theorem 1. Consider the update equation (15), where $\lambda_\mu \in (0,1)$ and each ξ_i evolves according to (7). Then, we have

$$\lim_{k\to\infty} \mu_{ij}(t_k) = \beta_{ij} \tag{16}$$

where t_k implies the instants of updating, $\mu_{ij}(0) = \mu(0)$.

Proof. Considering the fact that $\beta_{ij} = \frac{\xi_j(t_2)-\xi_j(t_1)}{\xi_i(t_2)-\xi_i(t_1)}$ regardless of the two instants t_1 and t_2, it is easy to know that $\mu_{ij}(t_k) = \lambda_\mu^k\mu(0)+\sum_{l=1}^{k-1}(1-\lambda_\mu)^l\beta_{ij} = \lambda_\mu^k\mu(0)+\beta_{ij}(1-\lambda_\mu^k)$. Since $\lambda_\mu \in (0,1)$, we take the limit for $k\to\infty$. Therefore, Theorem 1 is completed. □

Remark 4. The quantity β_{ij} is time-varying, and affected by noise. So, it is not necessary to perform the update at a fixed frequency.

3.1.2 Clock skew compensation

Usually in practice, every clock node bootstraps each other till all of them converge to a global value. In detail, every clock node stores its own "virtual" clock skew estimation $\hat{s}_i$, which is defined in (5). When the clock node i receives an information packet from node j, it updates $\hat{s}_i$ as follows:

$$\hat{s}_{i_{\text{new}}} = \lambda_\omega \hat{s}_i + (1-\lambda_\omega)\mu_{ij}\hat{s}_j \tag{17}$$

where $\hat{s}_j$ is the "virtual" clock skew estimation of the neighbor node j and $\hat{s}_i(0) = 1$. From (9), we can obtain an equivalent equation such that $\lim_{t\to\infty}\hat{s}_i\beta_i = \beta_v$. To do so, we define the useful variant $\Xi_i = \hat{s}_i\beta_i$. It is known that after an initial transient period of (16), we have $\mu_{ij} = \beta_{ij}$. Also, if we multiply all the terms in (17) by β_i, then it can be presented as the following:

$$\Xi_{i_{\text{new}}} = \lambda_\omega \Xi_i + (1-\lambda_\omega)\Xi_j \tag{18}$$

In the sequel, we use a summary of several results related to the necessary and sufficient conditions[7, 23] to show the proposed skew estimation and compensation mechanism.

Theorem 2. Consider the update equation (17) with initial condition $\hat{s}_i(0) = 1$ and $\lambda_\mu \in (0,1)$. Also assume that $\mu_{ij} = \beta_{ij}$ for all i,j and the communication graph of dynamical systems $\mathcal{G}$ is strongly connected. Then,

$$\lim_{t\to\infty} \hat{s}_i(t)\beta_i = \beta_v, \quad \forall i \tag{19}$$

where β_v is a constant parameter satisfying the condition $\beta_v \in [\min_i(\beta_i(0)), \max_i(\beta_i(0))]$.

Proof. Let $\Xi(t) = (\Xi_1(t), \Xi_2(t), \cdots, \Xi_n(t))^{\rm T}$, $\Xi_i(t) = \beta_i\hat{s}_i(t)$, and $\boldsymbol{e} = (1,1,\cdots,1)^{\rm T}$. Consider the time sequence $t_p = pT$, where T is the length of time window. Let ς_h^p denotes the district ordered communication instants of all the clock nodes within $t \in [t_p, t_{p+1})$. Let $j_{\varsigma_p,h}$ transmits its $\hat{s}_j$ which is described in (17) at the time instant $j_{\varsigma_p,h}$ and all its neighbors receive the message which updates their $\hat{s}_i$ according to (17). Then, we define a time varying stochastic matrix $A_{\varsigma_p,h}$, which has some important properties given in [18] such matrix depends on nodes that are exchanging synchronization messages such that all are zeros except for $[A_{\varsigma_p,h}]_{i,j_{\varsigma_p,h}} = 1-\lambda_\omega$ and $[A_{\varsigma_p,h}]_{i,i} = \lambda_\omega$, where i is a neighbor of $j_{\varsigma_p,h}$. According to this terminology, it can be described as $\Xi(t_{p+1}) = A_{\varsigma_p,h_p}A_{\varsigma_p,h_p-1}\cdots A_{\varsigma_p,2}A_{\varsigma_p,1}\Xi(t_p) = A_p\Xi(t_p)$. Because each clock node communicates at least once in the p-th time window, where $t\in[t_p,t_{p+1})$, we know from [23] that A_p is strongly connected and also rooted at some node ω independent of p. Now, define the new time sequence $\bar{t}_q = qnT$, then we get the following form: $\Xi(\bar{t}_{q+1}) = A_{qn+n-1}\cdots A_{qn+1}A_{qn}\Xi(\bar{t}) = \bar{A}_q\Xi(\bar{t})$. According to the proposition in [23], the graph corresponding to the matrices $\bar{A}_q$ is strongly rooted at the same node ω, which is a sufficient condition[7] to ensure that: $\lim_{t\to\infty}\Xi(t) = \lim_{q\to\infty}\Xi(t_q) = \prod_{m=1}^{\infty}\bar{A}_m\Xi(0) = \Xi_{ss}\mathrm{e}$, where $\Xi_{ss} \in \mathbf{R}$. Because all $\bar{A}_m, m = 1,2,\cdots$ are stochastic, we can get $\max(\bar{A}_m\Xi) \le \max(\Xi)$ and $\min(\bar{A}_m\Xi) \ge \min(\Xi)$, from which it follows that $\Xi_{ss}\in[\min(\Xi(0)),\max(\Xi(0))]$. Having $\Xi_i(t) = \beta_i\hat{s}_i(t)$ and $\Xi_i(0) = \beta_i\hat{s}_i(0)$, we prove the Theorem 2. □

Remark 5. It is known that the algorithm does not depend on exact time instants at which the nodes transmit as long as they transmit from time to time. The only important condition is that the graph must be sufficiently connected and strongly rooted, which implies that FASA is robust to link failure and packet collision.

3.1.3 Clock offset compensation

According to the previous analysis, after the clock skew compensation based on FASA is applied, all "virtual" clock estimators have the same skews. So (8) can be written as:

$$\hat{\xi}_i(t) = \beta_v t + \frac{\beta_v}{\beta_i}\alpha_i + \hat{o}_i \tag{20}$$

It is also necessary to compensate the possible clock offset errors. By FASA, we update the "virtual" clock offset (5) as follows:

$$\hat{o}_{i_{\text{new}}} = \hat{o}_i + (1-\lambda_o)(\hat{\xi}_j - \hat{\xi}_i) = \hat{o}_i + (1-\lambda_o)(\hat{s}_j\xi_j + \hat{o}_j - \hat{s}_i\xi_i - \hat{o}_i) \tag{21}$$

where ξ_j and ξ_i are computed at the same time instant. According to (10), we need to know whether the clock offset update equation guarantees $\alpha_v = \lim_{t\to\infty}(\hat{o}_i + \beta_v/\beta_i\cdot\alpha_i)$ for all clock nodes, where $\lambda_o\in(0,1)$. To simplify the problem, let $\Omega_i = (\hat{o}_i + \beta_v/\beta_i\cdot\alpha_i)$; if we substitute (20) into (21), we get the following equation:

$$\Omega_{i_{\text{new}}} = \lambda_o\Omega_i + (1-\lambda_o)\Omega_j \tag{22}$$

It is observed that (22) has the same structure as (21). Hence, under the same hypotheses of Theorem 2, all $\Omega_i, i = 1,2,\cdots,n$ will converge to the same value.

Remark 6. From above, it is clear that FASA includes three main steps, which are shown in (15), (18), and (22). First, FASA estimates for each clock the relative skew with respect to its neighbors, and then, each node updates its value by averaging it relative to the estimate of its neighbors. Finally, when all the clock nodes have the same skews, we use FASA to update the clock offset. Following this course, all the clock nodes in dynamical network will be synchronized soon via FASA.

3.2 Convergence analysis

Because of the dynamic behavior of FASA, we adopt compartmental system model which is defined in (14) to characterize FASA. In this section, we will prove that such dynamical system with time-delays accords with the requirements of semistable. To begin with, one presents a rigorous mathematical definition for the network synchronization.

Definition 4. If there is a nonempty subset $D\subseteq\mathbf{R}$ with $\xi_0(t)\in D$, such that $\xi(t)\in\mathbf{R}$ for all $t\ge 0$, and

$$\lim_{t\to\infty}\|\xi_i(t)-\xi_v(t)\| = 0, \quad 1\le i\le n \tag{23}$$

then the dynamical network $\mathcal{G}$ is said to achieve network synchronization and $D \times \cdots \times D$ is called the region of synchrony for the dynamical network.

Note that for addressing the stability of the zero solution to a time-delayed nonnegative system, the usual stability definitions given in [16, 24−25] need to be slightly modified. In fact, the system needs to be defined with respect to relatively open subsets of $\bar{\mathbf{R}}_+^n$ containing the equilibrium solution $\xi_i(t) = 0$. According to a similar definition in [13], standard Lyapunov stability definition for nonlinear time-delayed system, which is mentioned in [16], can be used directly with the required sufficient condition verified on $\bar{\mathbf{R}}_+^n$. The following definitions generalize the notions of nonnegativity to vector fields.

Definition 5[13]**.** $\boldsymbol{f}$ is essentially nonnegative if $\boldsymbol{f}_i(\boldsymbol{\xi}) \geq 0$ for all $i = 1, \cdots, n$ and $\boldsymbol{\xi}(t) \in \bar{\mathbf{R}}_+^n$ such that $\xi_i(t) = 0$, where $\boldsymbol{f} = [\boldsymbol{f}_1, \boldsymbol{f}_2, \cdots, \boldsymbol{f}_n]^{\mathrm{T}} : \mathcal{H} \to \mathbf{R}^n$, and $\mathcal{H}$ is an open subset of $\mathbf{R}^n$ that contains $\bar{\mathbf{R}}_+^n$.

Definition 6[26]**.** Consider the nonlinear time-delayed dynamical system given by (11). If $\boldsymbol{f}(\cdot)$ is essentially nonnegative and $\boldsymbol{f}_d(\cdot)$ is nonnegative so that every $\boldsymbol{\phi}(\cdot) \in \mathbf{C}_+, \mathbf{C}_+ = \{\varphi(\cdot) \in \mathbf{C} : \varphi(\theta) \geq 0, \theta \in [-\tau^*, 0]\}$, then the solution $\xi_i(t)$ with $t \geq 0$ and $\mathcal{G}$ are nonnegative.

Lemma 1[26]**.** If $\boldsymbol{e}^{\mathrm{T}}(\boldsymbol{f}(\boldsymbol{\xi}) + \sum_{i=1}^{n_d} \boldsymbol{f}_{d_i}(\boldsymbol{\xi})) = 0$, there exist nonnegative diagonal matrices $Q_i \in \bar{\mathbf{R}}_+^{n\times n}$, such that $Q = \sum_{i=1}^{n_d} Q_i > 0$,

$$Q_i^D Q_i \boldsymbol{f}_{d_i}(\boldsymbol{\xi}) = \boldsymbol{f}_{d_i}(\boldsymbol{\xi}), \quad \boldsymbol{\xi} \in \bar{\mathbf{R}}_+^n, \quad i = 1, \cdots, n_d \tag{24}$$

$$\sum_{i=1}^{n_d} \boldsymbol{f}_{d_i}^{\mathrm{T}}(\boldsymbol{\xi}) Q_i \boldsymbol{f}_{d_i}(\boldsymbol{\xi}) \leq \boldsymbol{f}^{\mathrm{T}}(\boldsymbol{\xi}) Q \boldsymbol{f}(\boldsymbol{\xi}), \quad \boldsymbol{\xi} \in \bar{\mathbf{R}}_+^n \tag{25}$$

Theorem 3. Consider the nonlinear dynamical network system with time-delays given by (14). If $\boldsymbol{f}(\boldsymbol{\xi}) + \sum_{i=1}^{n_d} \boldsymbol{f}_{d_i}(\boldsymbol{\xi}) = 0, \boldsymbol{\xi} \in \bar{\mathbf{R}}_+^n$, then for any $M \geq 0, M \cdot \boldsymbol{e}$ is a semistable equilibrium point. That is, $\lim_{t\to\infty} \Xi(t) = M^* \cdot \boldsymbol{e}$ and it has the same meaning as (26) and M^* satisfies

$$nM^* + \sum_{i=1}^{n_d} \tau_i^* \boldsymbol{e}^{\mathrm{T}} \boldsymbol{f}_{d_i}(M^* \boldsymbol{e}) = \boldsymbol{e}^{\mathrm{T}} \boldsymbol{\phi}(0) + \sum_{i=1}^{n_d} \int_{-\tau_i}^{0} \boldsymbol{e}^{\mathrm{T}} \boldsymbol{f}_{d_i}(\boldsymbol{\phi}(\theta)) \mathrm{d}\theta \tag{26}$$

Proof. Consider the Lyapunov function V: $\mathbf{C}_+ \to \mathbf{R}$ is given by $V(\zeta(\cdot)) = -\sum_{i=1}^{n} \int_0^{\zeta_i(0)} Q_{(i,i)} \boldsymbol{f}_i(\vartheta) \mathrm{d}\vartheta + \sum_{i=1}^{n_d} \int_{-\tau_i}^{0} \boldsymbol{f}_{d_i}^{\mathrm{T}}(\zeta(\theta)) Q_i \boldsymbol{f}_{d_i}(\zeta(\theta)) \mathrm{d}\theta$. It follows that $v(\zeta) \geq \sum_{i=1}^{n} Q_{(i,i)}[-\boldsymbol{f}_i(\delta_i \zeta_i(0))]\zeta_i(0) > 0$ for all $\zeta(0) \neq 0$, where $0 < \delta_i < 1$. Because $\boldsymbol{f}_i(\cdot)$ is a strictly decreasing function, there exists a class κ function $M(\cdot)$ such that $V(\zeta) > M(\|\zeta(0)\|)$. The derivative of $V(\boldsymbol{\xi}_t)$ along the trajectories of (14) is

$$\begin{aligned}
&\dot{V}(\xi(t)) = -\boldsymbol{f}^{\mathrm{T}}(\boldsymbol{\xi}(t) Q \dot{\boldsymbol{\xi}}(t)) + \sum_{i=1}^{n_d} \boldsymbol{f}_{d_i}^{\mathrm{T}}(\boldsymbol{\xi}(t)) Q_i \boldsymbol{f}_{d_i}(\boldsymbol{\xi}(t)) - \\
&\sum_{i=1}^{n_d} \boldsymbol{f}_{d_i}^{\mathrm{T}}(\boldsymbol{\xi}(t-\tau_i)) Q_i \boldsymbol{f}_{d_i}(\boldsymbol{\xi}(t-\tau_i)) = \\
&-\boldsymbol{f}^{\mathrm{T}}(\boldsymbol{\xi}(t)) Q \boldsymbol{f}(\boldsymbol{\xi}(t)) - \sum_{i=1}^{n_d} \boldsymbol{f}^{\mathrm{T}}(\boldsymbol{\xi}(t)) Q \boldsymbol{f}_{d_i}(\boldsymbol{\xi}(t-\tau_i)) + \\
&\sum_{i=1}^{n_d} \boldsymbol{f}_{d_i}^{\mathrm{T}}(\boldsymbol{\xi}(t)) Q_i \boldsymbol{f}_{d_i}(\boldsymbol{\xi}(t)) - \\
&\sum_{i=1}^{n_d} \boldsymbol{f}_{d_i}^{\mathrm{T}}(\boldsymbol{\xi}(t-\tau_i)) Q_i \boldsymbol{f}_{d_i}(\boldsymbol{\xi}(t-\tau_i)) \leq \\
&-\boldsymbol{f}^{\mathrm{T}}(\boldsymbol{\xi}(t)) Q \boldsymbol{f}(\boldsymbol{\xi}(t)) - \sum_{i=1}^{n_d} \boldsymbol{f}^{\mathrm{T}}(\boldsymbol{\xi}(t)) Q Q_i^D Q_i \boldsymbol{f}_{d_i}(\boldsymbol{\xi}(t-\tau_i)) - \\
&\sum_{i=1}^{n_d} \boldsymbol{f}_{d_i}^{\mathrm{T}}(\boldsymbol{\xi}(t-\tau_i)) Q_i Q_i^D Q_i \boldsymbol{f}_{d_i}(\boldsymbol{\xi}(t-\tau_i)) - \\
&\sum_{i=1}^{n_d} [Q\boldsymbol{f}(\boldsymbol{\xi}(t)) + Q_i \boldsymbol{f}_{d_i}(\boldsymbol{\xi}(t-\tau_i))]^{\mathrm{T}} \times \\
&Q_i^D [Q\boldsymbol{f}(\boldsymbol{\xi}(t)) + Q_i \boldsymbol{f}_{d_i}(\boldsymbol{\xi}(t-\tau_i))] \leq 0, \quad t \geq 0
\end{aligned}$$

where the first inequality follows from (24) and (25) in Lemma 1, and the last equality follows the fact that $\boldsymbol{f}^{\mathrm{T}}(\boldsymbol{\xi}) Q \boldsymbol{f}(\boldsymbol{\xi}) = \sum_{i=1}^{n_d} \boldsymbol{f}^{\mathrm{T}}(\boldsymbol{\xi}) Q Q_i^D Q \boldsymbol{f}(\xi)$, $\xi \in \bar{\mathbf{R}}_+^n$. Let $\mathcal{P} = \{\zeta(\cdot) \in \mathbf{C}_+ : Q\boldsymbol{f}(\zeta(0)) + Q_i \boldsymbol{f}_{d_i}(\zeta(-\tau_i)) = 0, i = 1, \cdots, n_d\}$, and since the positive orbit $\rho^+(\boldsymbol{\phi}(\theta))$ of (14) is bounded, where $\rho^+(\boldsymbol{\phi}(\theta)) \in \mathbf{C}_+$. From the theorem in [16], we know that $\lim_{t\to\infty} \boldsymbol{\xi}(t) = \hat{\mathcal{P}}$. Then, we consider the following function $\mathcal{W} : \mathbf{C}_+ \to \mathbf{R}$ by $\mathcal{W}(\zeta(\cdot)) = \boldsymbol{e}^{\mathrm{T}} \boldsymbol{\phi}(0) + \sum_{i=1}^{n_d} \int_{-\tau_i}^{0} \boldsymbol{e}^{\mathrm{T}} f_{d_i}(\boldsymbol{\phi}(\theta)) \mathrm{d}\theta$. Thus, for all $t \geq 0$, along the trajectories of (14): $\mathcal{W}(\xi(t)) = \mathcal{W}(\boldsymbol{\phi}(\cdot)) = \boldsymbol{e}^{\mathrm{T}} \boldsymbol{\phi}(0) + \sum_{i=1}^{n_d} \int_{-\tau_i}^{0} \boldsymbol{e}^{\mathrm{T}} \boldsymbol{f}_{d_i}(\boldsymbol{\phi}(\theta)) \mathrm{d}\theta$, which implies that $\boldsymbol{\xi}(t) \to \hat{\mathcal{P}} \cap \mathcal{T}$, where $\mathcal{T} = \{\zeta(\cdot) \in \mathbf{C}_+ : \mathcal{W}(\zeta(\cdot)) = \mathcal{W}(\boldsymbol{\phi}(\cdot))\}$. Hence, $\hat{\mathcal{P}} \cap \mathcal{T} = \{M^* \cdot \boldsymbol{e}\}$, and $\lim_{t\to\infty} \boldsymbol{\xi}(t) = M^* \cdot \boldsymbol{e}$, where M^* satisfies (26). Finally, we consider the following Lyapunov function $V(\zeta(\cdot)) = -\sum_{i=1}^{n} \int_M^{\zeta_i(0)} Q_{(i,i)}(\boldsymbol{f}_i(\vartheta) - \boldsymbol{f}_i(M)) \mathrm{d}\vartheta + \sum_{i=1}^{n_d} \int_{-\tau_i}^{0} [\boldsymbol{f}_{d_i}(\zeta(\theta)) - \boldsymbol{f}_{d_i}(M\boldsymbol{e})]^{\mathrm{T}} Q_i [\boldsymbol{f}_{d_i}(\zeta(\theta)) - \boldsymbol{f}_{d_i}(M\boldsymbol{e})] \mathrm{d}\theta$, and noting that $V(\zeta) \geq \sum_{i=1}^{n_d} Q_{(i,i)}[\boldsymbol{f}_i(M) - \boldsymbol{f}_i(M + \delta_i(\zeta_i(0) - M))] \cdot (\zeta_i(0) - M) > 0$, for all $\zeta_i(0) \neq M$, where $0 < \delta_i < 1$. So $M \cdot \boldsymbol{e}$, $M \geq 0$ is a semistable equilibrium point of (14). □

Remark 7. Theorem 3 characterizes the operating process of FASA and establishes the semistability for the special case of nonlinear dynamical system of the form (14) where $\boldsymbol{f}(\cdot)$ and $\boldsymbol{f}_d(\cdot)$, $i = 1, \cdots, n$ satisfy (13), (24), and (25).

4 Simulation and experimental results

The experimental facilities which are often called inverse GPS (IGPS) base station network[27] are shown in Fig. 3. Each clock node is equipped with an external oscillator running at 5 MHz frequency which has a granularity of about 10 ns per tic. The communication time-delays between every clock nodes are measured through electric wires.

And then, consider the vector figure in Fig. 4 which is corresponding to the real system in Fig. 3. Here, we choose the values $\mathcal{V} = \{1, 2, 3, 4\}$, $\mathcal{E} = \{(1, 2), (2, 3), (3, 4), (4, 3), (4, 1)\}$ with adjacency matrix $\mathcal{A}$ such that $a_{21} > 0$, $a_{34} > 0$, $a_{43} > 0$, and $a_{14} > 0$, and with the remaining elements being zeros.

In this case, the input to the network is given by: $\boldsymbol{u}_1(t) = \boldsymbol{f}_1(\xi_1(t), \xi_4(t-\tau_{14}))$, $\boldsymbol{u}_2(t) = \boldsymbol{f}_2(\xi_2(t), \xi_1(t-\tau_{21}))$, $\boldsymbol{u}_3(t) = \boldsymbol{f}_3(\xi_3(t), \xi_2(t-\tau_{32}), \xi_4(t-\tau_{34}))$, $\boldsymbol{u}_4(t) = \boldsymbol{f}_4(\xi_4(t), \xi_1(t-\tau_{43}))$. For i=1, 2, 3, 4, $\dot{\xi}_i(t)$ is only dependent on the states of the clock nodes that are accessible by clock node i and with τ_{ij}. After every one second, an external standard oscillator node simultaneously inquire the four synchronizing clock nodes of their estimated virtual time $\hat{\xi}_i$. From Section 1, we know that DTSP[12] is similar to our FASA.

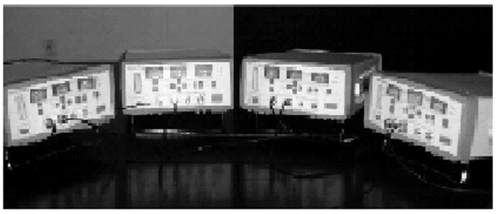

Fig. 3 The experimental facilities of IGPS base station network with time-delays

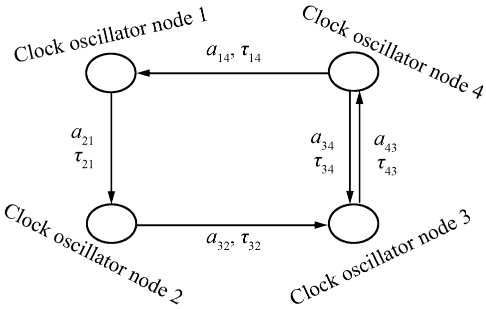

Fig. 4 Vector figure of nonlinear dynamical network with time-delays of four clock oscillator nodes

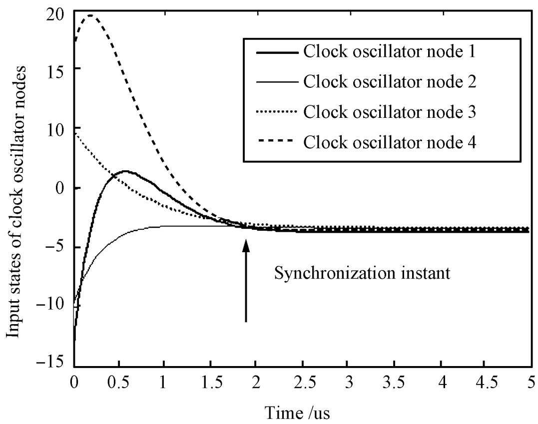

(a) State trajectories of clock nodes based on FASA

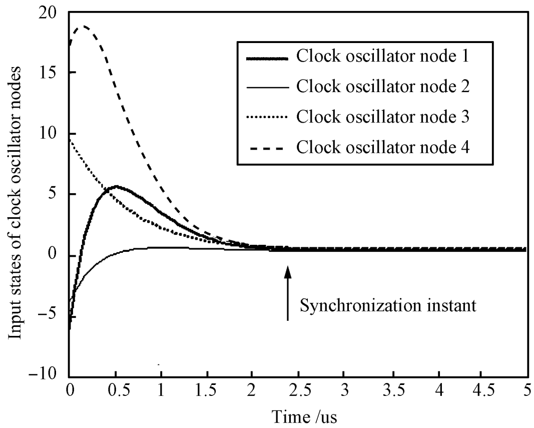

(b) State trajectories of clock nodes based on DTSP

Fig. 5 State trajectories of clock oscillator nodes based on two different algorithms

As a result, in the first simulation experiment using Matlab, we test the FASA compared with the DTSP to cope with dynamical network changes of four oscillator nodes. We choose the initial input states of four oscillator nodes as $\boldsymbol{\xi}_o = [-9, -5, 10, 16]^{\mathrm{T}}$ and $a_{ij} = 1$, $\tau_{ij} = 1\,s$, if $(i, j) \in \mathcal{E}$. Two different methods are adopted when four clock oscillator nodes are utilized. The synchronous value of clock oscillator nodes is determined solely by the communication topologies and initial state. With the passage of time, all oscillator nodes learn their neighbors information and use the information to improve their performance. After a period of time, all nodes are placed close to each other and they rapidly become synchronized. Fig. 5 (a) shows the state trajectories of four clock oscillator nodes using FASA, and that of the method presented in [12] is illustrated in Fig. 5 (b).

It is observed that the synchronization time in Fig. 5 (a) is evidently shorter than that in Fig. 5 (b), which means that the performance of FASA is superior to DTSP.

In the second simulation experiment, we test the performance of the FASA to find the clock skews and offsets with the communication of random time-delays. We use $\lambda_\mu = 0.25$, $\lambda_\omega = 0.2$, $\lambda_o = 0.3$, and $a_{ij} = 1$ if $(i, j) \in \mathcal{E}$ in the following simulations cases all the time. First, we plot the error between each oscillator $\hat{\xi}_i(t)$ from the node instantaneous mean, which is shown in Fig. 6.

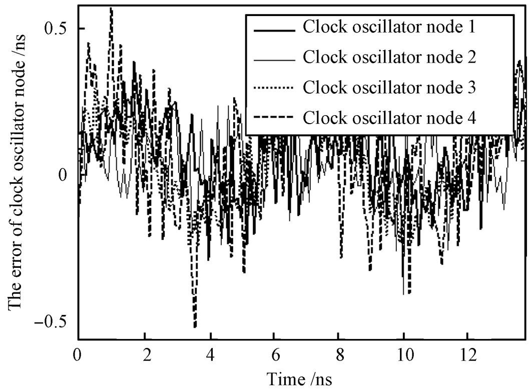

Fig. 6 Errors between four clock oscillator nodes from their instantaneous means (1 tic $\approx$ 10 ns)

It is obvious that due to measurement and quantization errors, the estimator shows very small errors, which is comparable to the maximum resolution limited by quantization error. Then, we consider cases in different communication time-delays.

The results shown in Figs. 7 (a) and (b) and Figs. 8 (a) and (b) are the clock oscillator skew and offset estimations by FASA with the communication delay $\tau_{ij} = 0.5\,\mathrm{s}$. Figs. 9 (a) and (b) present the results by FASA with the communication delay $\tau_{ij} = 2.5\,\mathrm{s}$.

From the simulation results, it is evident that we can get synchronization eventually from the mechanisms of clock skew and offset compensation by FASA. The offset and skew compensation mechanisms initially reduce the offsets and skews, but the different clock oscillator offsets and skews show the typical saw-tooth behavior as mentioned in Section 3. Furthermore, it is observed that errors between four clock oscillator nodes are close to the communication delays in nonlinear dynamical network. The errors in case of longer time delays are larger than those in smaller ones.

In the last experiment, we present the example where it is shown that the reading value of each clock synchronizes to the reading value of "virtual" reference clock by using FASA. We have preset the reading value at 50 Hz frequency and 100 μs pulse width in the "virtual" reference clock (Fig. 10), and then we install the FASA programme in each oscillator facility. Each oscillator facility exchanges its information with the others. After 1.7 s, we can find that the reading of each oscillator facility is almost the same as the preset reading which is shown in Fig. 11.

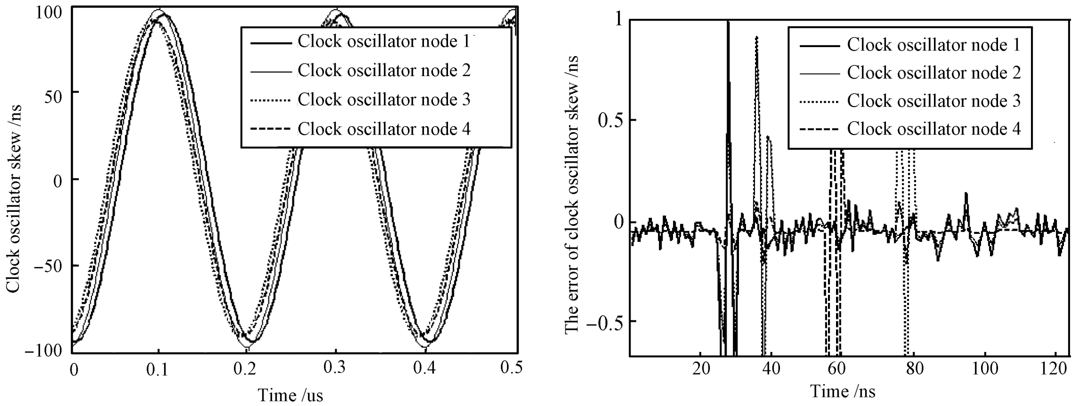

(a) The skew estimation $\hat{s}_i$ of each clock oscillator (b) Errors between four clock skews

Fig. 7 Clock skew estimation and error by using FASA algorithm with $\tau_{ij} = 0.5\,\text{s}$, $i, j = 1, 2, 3, 4$

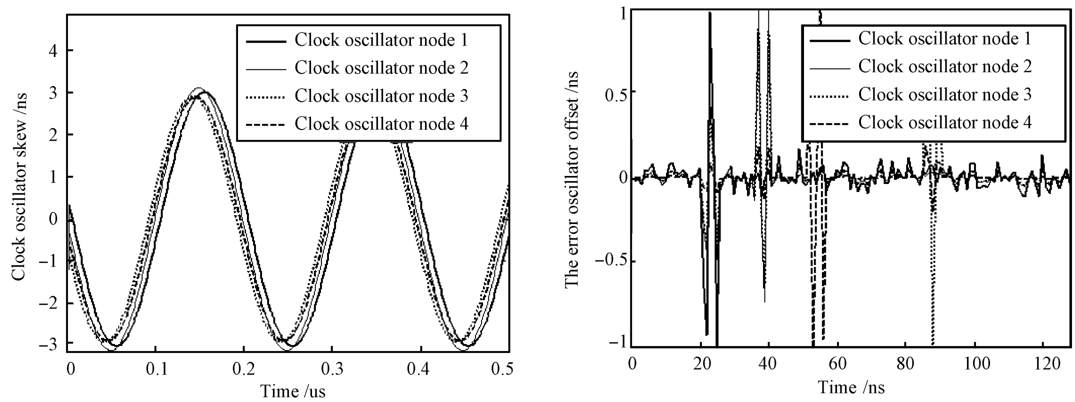

(a) The offset estimation $\hat{o}_i$ of each clock oscillator (b) Errors between four clock offsets

Fig. 8 Clock oscillator offset estimation and errors by using FASA algorithm with $\tau_{ij} = 0.5\,\text{s}$, $i, j = 1, 2, 3, 4$

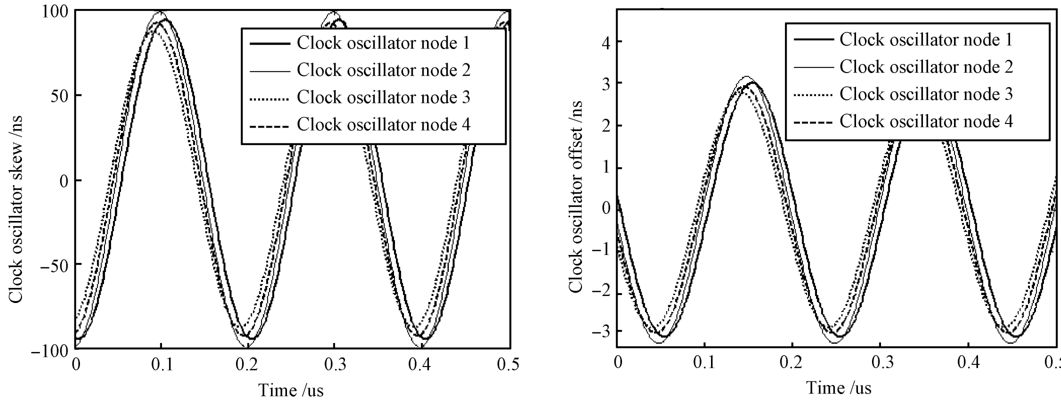

(a) The skew estimation $\hat{s}_i$ of each clock oscillator (b) The skew estimation $\hat{o}_i$ of each clock oscillator

Fig. 9 Clock oscillator skew and offset estimation by FASA algorithm with $\tau_{ij} = 2.5\,\text{s}$, $i, j = 1, 2, 3, 4$

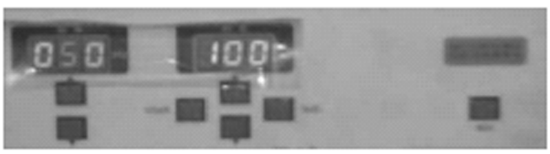

Fig. 10 The preset reading of "virtual" reference clock

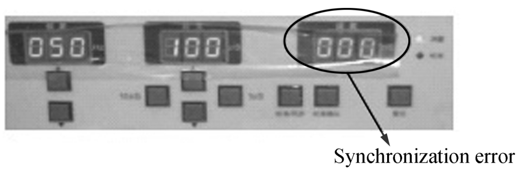

Fig. 11 The reading of each clock oscillator facility

5 Conclusion

The synchronization problem of clock oscillator nodes coupled with the nonlinear dynamical network with random time-delays was investigated in this paper. A novel synchronization algorithm, the fast averaging synchronization algorithm (FASA), is proposed, which is fully distributed, online, and global, including the clock skew estimation, skew compensation, and offset compensation. The dynamic algorithm is characterized by compartmental system with time-delays and we find the Lyapunov asymptotic stable equilibrium of the dynamical network in order to prove the convergence of FASA. The comparison between FASA and the powerful DTSP method also indicates the superiority of our proposed method. FASA has been successfully applied to the dynamical network with time-delays of IGPS base stations. It is also observed that FASA works well when a network has to be swiftly synchronized.

References

1 Hoppensteadt F C, Izhikevich E M. Associative memory of weakly connected oscillators. In: Proceedings of the International Conference on Neural Networks. Houston, USA: Springer, 1997. 1135−1138

2 Pikovsky A, Rosenblum M, Kurths J. *Synchronization: A Universal Concept in Nonlinear Sciences*. Cambridge: Cambridge University Press, 2001

3 Boyd S, Ghosh A, Prabhakar B, Shah D. Gossip algorithms: design, analysis and applications. In: Proceedings of the 24th Annual Joint Conference of the IEEE Computer and Communications Societies. Piscataway, USA: IEEE, 2005. 1653−1664

4 Savkin A V. Coordinated collective motion of groups of autonomous mobile robots: analysis of Vicsek′s model. *IEEE Transactions on Automatic Control*, 2004, **49**(6): 981−989

5 Yu L, Wang H B, Kuo G S, Cheng S D, Qi L. A fuzzy-based approach to remove clock skew and reset from one-way delay measurement. *IEEE Transactions on Neural Networks*, 2005, **16**(5): 1125−1135

6 Xiao F, Wang L. Asynchronous consensus in continuous-time multi-agent systems with switching topology and time-varying delays. *IEEE Transactions on Automation Control*, 2008, **53**(8): 1804−1816

7 Olfati S R, Fax J A, Murray R M. Consensus and cooperation in networked multi-agent systems. *Proceedings of the IEEE*, 2007, **95**(1): 215−233

8 Papachristodoulou A, Jadbabaie A. Synchronization in oscillator networks: switching topologies and non-homogeneous delays. In: Proceedings of the 44th IEEE Conference on Decision and Control. Seville, Spain: IEEE, 2005. 5692−5697

9 Olfati S R, Murray R M. Consensus problems in networks of agents with switching topology and time-delays. *IEEE Transactions on Automatic Control*, 2004, **49**(9): 1520−1533

10 Elson J, Girod L, Estrin D. Fine-grained network time synchronization using reference broadcasts. In: Proceedings of the 5th Symposium on Operating Systems Design and Implementation. Boston, USA: IEEE, 2002. 147−163

11 Werner A G, Tewari G, Patel A, Welsh M, Nagpal R. Firefly-inspired sensor network synchronicity with realistic radio effects. In: Proceedings of the 3rd International Conference on Embedded Networked Sensor Systems. San Diego, USA: ACM, 2005. 142−153

12 Solis R, Borkar V S, Kumar P R. A new distributed time synchronization protocol for multihop wireless networks. In: Proceedings of the 45th IEEE Conference on Decision and Control. San Diego, USA: IEEE, 2006. 2734−2739

13 Haddad W M, Chellaboina V. Stability and dissipativity theory for nonnegative dynamical systems: a unified analysis framework for biological and physiological systems. *Nonlinear Analysis:Real World Applications*, 2005, **6**(1): 35−65

14 Bernstein D C, Hyland D C. Compartmental modeling and second-moment analysis of state space systems. *SIAM Journal on Matrix Analysis and Applications*, 1993, **14**(3): 880−901

15 Sandberg I. On the mathematical foundations of compartmental analysis in biology, medicine, and ecology. *IEEE Transactions on Circuits and Systems*, 1978, **25**(5): 273−279

16 Hale J K, Lunel S M. *Introduction to Functional Differential Equations*. New York: Springer-Verlag, 1993. 98−142, 146−232

17 Olfati S R, Murray R M. Consensus problems in networks of agents with switching topology and time-delays. *IEEE Transactions on Automatic Control*, 2004, **49**(9): 1520−1533

18 Boyd S, Ghosh A, Prabhakar B, Shah D. Randomized gossip algorithms. *IEEE/ACM Transactions on Networking*, 2006, **14**(S1): 2508−2530

19 Preciado V M, George C V. Synchronization in generalize Erdddotos-Racuteenyi networks of nonlinear oscillators. In: Proceedings of the 44th IEEE Conference on Decision and Control. Seville, Spain: IEEE, 2005. 4628−4633

20 Zhang L, Liu Z, Xia H H. Clock synchronization algorithms for network measurements. In: Proceedings of the 21st Annual Joint Conference of the IEEE Computer and Communications Societies. New York, USA: IEEE, 2002. 160−169

21 Moon S B. Measurement and Analysis of End-to-End Delay and Loss in the Internet [Ph. D. dissertation], University of Massachusetts, USA, 2000

22 Galleani L, Sacerdote L, Tavella P, Zucca C. A mathematical model for the atomic clock error. *Metrologia*, 2003, **40**(3): 257−264

23 Cao M, Morse A S, Anderson B D O. Reaching a consensus in a dynamically changing environment: a graphical approach. *SIAM Journal on Control and Optimization*, 2008, **47**(2): 575−600

24 Bernstein D S. *Matrix Mathematics*. Princeton: Princeton University Press, 2006. 120−223

25 Hale J K. Dynamical systems and stability. *Journal of Mathematical Analysis and Applications*, 1969, **26**(1): 39−59

26 Haddad W M, Chellaboina V. Stability theory for nonnegative and compartmental dynamical systems with time delay. *Systems and Control Letters*, 2004, **51**(5): 355−361

27 Yu M, Chen J, Dou L H, Gang M G. Positioning accuracy of IGPS. *Journal of Harbin Institute of Technology (New Series)*, 2010, **17**(2): 99−104

CHEN Jie Ph. D., professor at the School of Automation, Beijing Institute of Technology. From 1989 to 1990, he was a visiting scholar at California State University, USA. From 1996 to 1997, he was a research fellow at University of Birmingham, UK. His research interest covers multi-index optimization, multi-objective decision and control, intelligent control, and constrained nonlinear control. E-mail: chenjie@bit.edu.cn

YU Miao Ph. D. candidate at Beijing Institute of Technology. His research interest covers clock synchronization in nonlinear system and synchronization in distributed system. Corresponding author of this paper. E-mail: olivermiaoer@163.com

DOU Li-Hua Received her Ph. D. degree from Beijing Institute of Technology in 2000. She is currently a professor at the School of Automation, Beijing Institute of Technology. Her research interest covers complex system and intelligent control. E-mail: doulihua@bit.edu.cn

GAN Ming-Gang Received his Ph. D. degree from Beijing Institute of Technology in 2006. He is currently a lecturer at the School of Automation, Beijing Institute of Technology. His research interest covers complex system and synchronization of nonlinear system. E-mail: aganbit@126.com